SLAC-PUB-14455

A second-order achromat design based on FODO cell

Yipeng Sun (yisun@slac.stanford.edu)
SLAC, Stanford, CA 94025, USA

July 12, 2011

Abstract

Two dipole doglegs are widely used to translate the beam axis horizontally or vertically. Quadrupoles are placed between the two consecutive dipoles to match first order dispersion and provide betatron focusing. Similarly a four dipole chicane is usually employed to form a bypass region, where the beam axis is transversely shifted first, then translated back to the original axis. In order to generate an isochronous section, quadrupoles are again needed to tune the first order transfer matrix element R_{56} equaling zero. Usually sextupoles are needed to correct second order dispersion in the bending plane, for both the dogleg optics and the chicane (with quad) optics. In this paper, an alternative optics design is introduced, which is based on a simple FODO cell and does not need sextupoles assistance to form a second-order achromat. It may provide a similar function of either a dogleg or a bypass, by using 2 or 4 of such combined supercells.

1 Overview

A transverse dogleg beamline or a bypass beamline is needed for many accelerator systems from the requirement on shifting the beam axis in some region, which is sometimes due to realistic constraints. Some of these constraints are: existing infrastructure on the original beam axis; upgrade of an old accelerator; multi-function linac which feeds several downstream beamlines, and so on. A special example which has wide applications is a Free Electron Laser driving linac. At the end of such an FEL linac the electron beam can be used to feed several different undulators to generate photons for different purposes. There are also other systems which make use of the dispersion generated in the bending plane to do a momentum collimation on the beam and to remove the halo particles. In 1970s K. Brown developed a systematic approach to design second order achromats from investigating matrices formulae [1], which uses at least four identical cells with dipoles, quadrupoles and sextupoles and can eliminate all geomeric and chromatic terms up to second order. Then W. Wan developed another approach with Lie algebra to design achromat to arbitrary order, taking advantage of the midplane symmetry and using multipole magnets for each order (for example, octupoles for third order achromat) [2]. Usually these systems are designed with dipoles, quadrupoles and sextupoles, to zero both first order and second order dispersion in the bending plane, and to provide an isochronous transfer system in the bypass case. Generally the use of sextupole magnets implies a strict tolerance on the beamline alignments.

Work supported in part by US Department of Energy contract DE-AC02-76SF00515.

At the same time, in many of these beamlines, the electron beam is transported with a large energy spread which is in the percent level. To transport such a beam through the dogleg (or bypass) and preserve the transverse emittance at the same time is a difficult task. In the following sections, a FODO cell based optics design is described which eliminates the use of sextupoles. In one supercell, both the first order (R_{16} and R_{26}) and second order dispersion (T_{166} and T_{266}) terms are closed, which guarantees no chromatic emittance growth as the beam transports through this section. Usually the initial transverse beam emittance is small in such systems being considered and one can neglect the small impact of the non-zero geometrical terms. Macro particle tracking simulations have been performed in the code Elegant [3], to evaluate the property of this optics design.

2 Equation of motion and matrix treatment

A moving coordinate system origined on the central trajectory of the beam line is employed here. Each particle in the beam has a coordinates of $(x, x', y, y', z, \delta_p)$. The divergence x' and y' are defined as the ratio of transverse momentum to longitudinal momentum. Without any approximations, the vector differential equation of motion is

$$\frac{d^2\mathbf{T}}{dT^2} = \frac{q}{p}\frac{d\mathbf{T}}{dT} \times \mathbf{B} \tag{1}$$

where $\mathbf{T}$ denotes the position vector of any particle moving along its trajectory, T the distrance travelled, q the particle charge and $\mathbf{B}$ the magnetic field.

With magnetic field expansion in three directions, the linearized (first order) differential equation of motion for the transverse coordinates x and y is [4]

$$x'' + (1-n)h^2 x = h\delta \tag{2}$$

$$y'' + nh^2 y = 0 \tag{3}$$

where $\delta = \Delta p/p_0$ denotes the relative momentum deviation from the on momentum particle, $h = B_y(0,0,t)/B\rho$ and the dimensionless parameter n given in terms of the vertical magnetic field component as shown in the following formula.

$$n = -\frac{1}{hB_y}\frac{\partial B_y}{\partial x}_{x=0,y=0} \tag{4}$$

Consider only the linear (first order) effect, after passing by a beam line, the final coordinates of any particle can be expressed by a linear function of its initial coordinates, as illustrated in the following formula.

$$x_1 = (x|x_0)x_0 + (x|x_0')x_0' + (x|\delta)\delta \tag{5}$$

where $(x|x_0)$ denotes the coefficient of x_0 in the equation for x_1, which is R_{11} in the following matrix formula.

Regarding the longitudinal motion, the path length difference depends on the initial coordinates $(x, x', y, y', z, \delta_p)$. From the vector differential equation of motion, the difference in path length of an arbitrary particle is calculated as an integral [4].

$$l = \int_0^t \left(\left[\left(\frac{dx}{d\tau} \right)^2 + \left(\frac{dy}{d\tau} \right)^2 + (1 + hx)^2 \right]^{\frac{1}{2}} - 1 \right) d\tau \tag{6}$$

The transport of particle's coordinates can be treated in a general matrix style as shown below.

$$\begin{pmatrix} x \\ x' \\ y \\ y' \\ z \\ \delta \end{pmatrix} = \mathbf{R} \cdot \begin{pmatrix} x_0 \\ x'_0 \\ y_0 \\ y'_0 \\ z_0 \\ \delta_0 \end{pmatrix} = \begin{pmatrix} R_{11} & R_{12} & R_{13} & R_{14} & R_{15} & R_{16} \\ R_{21} & R_{22} & R_{23} & R_{24} & R_{25} & R_{26} \\ R_{31} & R_{32} & R_{33} & R_{34} & R_{35} & R_{36} \\ R_{41} & R_{42} & R_{43} & R_{44} & R_{45} & R_{46} \\ R_{51} & R_{52} & R_{53} & R_{54} & R_{55} & R_{56} \\ R_{61} & R_{62} & R_{63} & R_{64} & R_{65} & R_{66} \end{pmatrix} \cdot \begin{pmatrix} x_0 \\ x'_0 \\ y_0 \\ y'_0 \\ z_0 \\ \delta_0 \end{pmatrix} \tag{7}$$

where $\mathbf{R}$ denotes the first order transport matrix of a beam line.

Given the magnetic field of a specified type of element, such as a dipole magnet, one can solve the linearized equation of motion and get the transfer matrix $\mathbf{R}$. Shown below are the first order transfer matrices of a dipole, a quadrupole, a sextupole and a drift, under thin lens approximation [4] [5]. Note that the discussion here is under the ultra relativistic condition.

The 6 by 6 transport matrix of the normal dipole magnet with bending angle θ and bending radius ρ can be written as

$$\mathbf{R}_{\mathbf{B}(\theta,\rho)} = \begin{pmatrix} \cos\theta & \rho\sin\theta & 0 & 0 & 0 & \rho(1-\cos\theta) \\ -\sin\theta/\rho & \cos\theta & 0 & 0 & 0 & \sin\theta \\ 0 & 0 & 1 & \rho\theta & 0 & 0 \\ 0 & 0 & 0 & 1 & 0 & 0 \\ -\sin\theta & \rho(\cos\theta - 1) & 0 & 0 & 1 & \rho(\sin\theta - \theta) \\ 0 & 0 & 0 & 0 & 0 & 1 \end{pmatrix} \tag{8}$$

The 6 by 6 transport matrix of a quadrupole magnet with integrated strength K_1 can be written as

$$\mathbf{R}_{\mathbf{Quad}} = \begin{pmatrix} 1 & L_Q & 0 & 0 & 0 & 0 \\ -K_1 & 1 & 0 & 0 & 0 & 0 \\ 0 & 0 & 1 & L_Q & 0 & 0 \\ 0 & 0 & K_1 & 1 & 0 & 0 \\ 0 & 0 & 0 & 0 & 1 & 0 \\ 0 & 0 & 0 & 0 & 0 & 1 \end{pmatrix} \tag{9}$$

The 6 by 6 transport matrix of a drift space with length L can be written as

$$\mathbf{R}_{\mathbf{Drift}} = \begin{pmatrix} 1 & L & 0 & 0 & 0 & 0 \\ 0 & 1 & 0 & 0 & 0 & 0 \\ 0 & 0 & 1 & L & 0 & 0 \\ 0 & 0 & 0 & 1 & 0 & 0 \\ 0 & 0 & 0 & 0 & 1 & 0 \\ 0 & 0 & 0 & 0 & 0 & 1 \end{pmatrix} \tag{10}$$

Sextupole is a type of second order magnetic element which does not change the first order optics. Its first order transport matrix is the same with a drift space of same length.

For monochromatic beams which occupies a very small phase space, first order transport matrix is a good approximation to describe the transmission properties of a beam line. For a realistic beam which usually has large energy spread, second order and higher order aberrations have to be taken in consideration. A general matrix notation for the transport of particles' coordinates is shown in the following formula, which has both first order and second order terms [4].

$$x_i(1) = \sum_j R_{ij} x_j(0) + \sum_{j,k} T_{ijk} x_j(0) x_k(0) \tag{11}$$

where second order matrix T has entries of the quadratic terms in the expansion of the final coordinates as a function of the initial coordinates.

To derive the second-order matrix elements for individual magnets, as has been done for the first order matrix, one need to again solve the equation of motion up to second order. Take a second order expansion in the transverse coordinates, and apply magnetic field expansion, the equation of motion is (rectangular coordinate system) [4]

$$x''+(1-n)h^2x = h\delta+(2n-1-\beta)h^3x^2+h'xx'+\frac{1}{2}hx'^2+(2-n)h^2x\delta+\frac{1}{2}(h''-nh^3+2\beta h^3)y^2+h'yy'-\frac{1}{2}hy'^2-h\delta^2 \tag{12}$$

$$y'' + nh^2y = 2(\beta - n)h^3xy + h'xy' - h'x'y + hx'y' + nh^2y\delta \tag{13}$$

A general solution of the above two differential equations consists of the solution of the homogeneous equation, and a particular solution of the inhomogeneous equation. The second order matrix element can be calculated as the Green's function integral of the associated driving term. The path length difference can be calculated using the same integration while retaining terms up to second order. Now, same as the calculation of the **R** (first order) matrices elements, one can calculate all the **T** (second order) matrices elements, given the magnetic field of a specified type of element, such as a quadrupole magnet. As discussed before, a drift space has no second order effects on the transport of particles' transverse coordinates. However, a drift does have two non-zero longitudinal **T** (second order) matrices elements, $T_{522,D} = T_{544,D} = -\frac{1}{2}L_D$. For a quadrupole magnet with integrated strength K_1 and length L_Q, its non-zero second order matrices elements are listed below.

$$T_{116,Q} = \frac{1}{2}K_1L_Q, T_{126,Q} = -\frac{1}{2}L_Q, T_{216,Q} = K_1, T_{226,Q} = \frac{1}{2}K_1L_Q \tag{14}$$

$$T_{336,Q} = -\frac{1}{2}K_1L_Q, T_{346,Q} = -\frac{1}{2}L_Q, T_{436,Q} = -K_1, T_{446,Q} = -\frac{1}{2}K_1L_Q \tag{15}$$

$$T_{512,Q} = \frac{1}{2}K_1L_Q, T_{522,Q} = -\frac{1}{2}L_Q, T_{534,Q} = -\frac{1}{2}K_1L_Q, T_{544,Q} = -\frac{1}{2}L_Q \tag{16}$$

For a sextupole magnet with integrated strength K_2 and length L_S, its non-zero second order matrices elements are listed below.

$$T_{111,S} = -\frac{1}{2}K_2L_S, T_{112,S} = -\frac{1}{3}K_2L_S^2, T_{122,S} = -\frac{1}{12}K_2L_S^3 \tag{17}$$

$$T_{133,S} = \frac{1}{2}K_2 L_S, T_{134,S} = \frac{1}{3}K_2 L_S^2, T_{144,S} = \frac{1}{12}K_2 L_S^3 \tag{18}$$

$$T_{211,S} = -K_2, T_{212,S} = -K_2 L_S, T_{222,S} = -\frac{1}{3}K_2 L_S^2 \tag{19}$$

$$T_{233,S} = K_2, T_{234,S} = K_2 L_S, T_{244,S} = \frac{1}{3}K_2 L_S^2 \tag{20}$$

$$T_{313,S} = K_2 L_S, T_{314,S} = \frac{1}{3}K_2 L_S^2, T_{323,S} = \frac{1}{3}K_2 L_S^2, T_{324,S} = \frac{1}{6}K_2 L_S^3 \tag{21}$$

$$T_{413,S} = 2K_2, T_{414,S} = K_2 L_S, T_{423,S} = K_2 L_S, T_{424,S} = \frac{2}{3}K_2 L_S^2 \tag{22}$$

$$T_{522,S} = -\frac{1}{2}L_S, T_{544,S} = -\frac{1}{2}L_S \tag{23}$$

For a dipole magnet with bending angle θ and bending radius ρ, its critical second order matrices elements are listed below.

$$T_{111,B} = -\frac{1}{2\rho}\sin^2\theta, T_{112,B} = \sin\theta\cos\theta, T_{122,B} = \frac{1}{2}\rho\cos\theta(1-\cos\theta) \tag{24}$$

$$T_{133,B} = 0, T_{134,B} = 0, T_{144,B} = -\frac{1}{2}\rho(1-\cos\theta) \tag{25}$$

$$T_{116,B} = \sin^2\theta, T_{126,B} = \rho\sin\theta(1-\cos\theta), T_{166,B} = -\frac{1}{2}\rho\sin^2\theta \tag{26}$$

$$T_{211,B} = 0, T_{212,B} = 0, T_{222,B} = -\frac{1}{2}\sin\theta \tag{27}$$

$$T_{233,B} = 0, T_{234,B} = 0, T_{244,B} = -\frac{1}{2}\sin\theta \tag{28}$$

$$T_{216,B} = \frac{\sin\theta}{\rho}, T_{226,B} = 0, T_{266,B} = -\sin\theta \tag{29}$$

$$T_{313,B} = 0, T_{314,B} = \sin\theta, T_{323,B} = 0, T_{324,B} = \rho(1-\cos\theta), T_{336,B} = 0, T_{346,B} = \rho\theta - \rho\sin\theta \tag{30}$$

$$T_{413,B} = 0, T_{414,B} = 0, T_{423,B} = 0, T_{424,B} = 0, T_{436,B} = 0, T_{446,B} = 0 \tag{31}$$

$$T_{511,B} = 0, T_{512,B} = 0, T_{522,B} = -\frac{1}{2}\rho\sin\theta \tag{32}$$

$$T_{533,B} = 0, T_{534,B} = 0, T_{544,B} = -\frac{1}{2}\rho\sin\theta \tag{33}$$

$$T_{516,B} = 0, T_{526,B} = -\rho(1-\cos\theta), T_{566,B} = 0 \tag{34}$$

Given known first order and second order transport matrices of all the magnetic elements in a lattice, one could multiply them subsequently to get the transport matrice of the whole system. As an example, for a lattice which consists of a dipole magnet, a drift and a quadrupole magnet, the overall transfer matrix reads (note the sequence of the multiplication)

$$\mathbf{R}_{all} = \mathbf{R}_{\mathbf{Quad}} \cdot \mathbf{R}_{\mathbf{Drift}} \cdot \mathbf{R}_{\mathbf{B}(\theta,\rho)} \tag{35}$$

$$\mathbf{T}_{all} = \mathbf{T}_{\mathbf{Quad}} \cdot \mathbf{T}_{\mathbf{Drift}} \cdot \mathbf{T}_{\mathbf{B}(\theta,\rho)} \tag{36}$$

To transport particle's coordinates through a beam line using up to second order matrices approach, in general one need a combined overall transport matrix which has 42-by-42 entries, which is reduced to 27-by-27 entries neglecting all the duplicated terms. In a simplified form (neglect all the zero and duplicated terms), the transport of the particle's coordinates in the bending plane is (up to second-order)

$$\begin{pmatrix} x \\ x' \\ z \\ \delta \\ x^2 \\ xx' \\ xz \\ x\delta \\ x'^2 \\ x'z \\ x'\delta \\ z^2 \\ z\delta \\ \delta^2 \\ y^2 \\ yy' \\ y'^2 \end{pmatrix} = \mathbf{T}_{\mathbf{x},[\mathbf{17}\times\mathbf{17}]} \cdot \begin{pmatrix} x_0 \\ x'_0 \\ z_0 \\ \delta_0 \\ x_0^2 \\ x_0 x'_0 \\ x_0 z_0 \\ x_0 \delta_0 \\ {x'_0}^2 \\ x'_0 z_0 \\ x'_0 \delta_0 \\ z_0^2 \\ z_0 \delta_0 \\ \delta_0^2 \\ y_0^2 \\ y_0 y'_0 \\ {y'_0}^2 \end{pmatrix} \tag{37}$$

The second-order transfer matrix in the bending plane can be expressed in the sub-matrix form of

$$\mathbf{T}_{\mathbf{x},[\mathbf{17}\times\mathbf{17}]} = \begin{pmatrix} \mathbf{T}_{\mathbf{11},[\mathbf{4}\times\mathbf{4}]} & \mathbf{T}_{\mathbf{12},[\mathbf{4}\times\mathbf{10}]} & \mathbf{T}_{\mathbf{13},[\mathbf{4}\times\mathbf{3}]} \\ \mathbf{0}_{[\mathbf{10}\times\mathbf{4}]} & \mathbf{T}_{\mathbf{22},[\mathbf{10}\times\mathbf{10}]} & \mathbf{0}_{[\mathbf{10}\times\mathbf{3}]} \\ \mathbf{0}_{[\mathbf{3}\times\mathbf{4}]} & \mathbf{0}_{[\mathbf{3}\times\mathbf{10}]} & \mathbf{T}_{\mathbf{33},[\mathbf{3}\times\mathbf{3}]} \end{pmatrix} \tag{38}$$

where $\mathbf{0}_{[\mathbf{3}\times\mathbf{6}]}$ denotes a three-by-six zero matrix, $\mathbf{T}_{\mathbf{22},[\mathbf{10}\times\mathbf{10}]}$ a ten-by-ten matrix, and all five sub-matrices are listed in Appendix. The transport of the particle's coordinates in the non-bending plane is much easier and not discussed in detail here.

3 First order optics

In this section, a standard FODO lattice is studied, to investigate the first order achromat condition and the associated relation between parameters of different magnets. A schematic plot of one super period which is composed of four identical standard FODO cells is shown in Figure 1. One FODO cell starts from a half focusing quadrupole with integrated strength K_{1f}, plus a drift with length l, followed by a dipole magnet with bending angle θ and bending radius ρ, another drift with same length and a full defocusing quadrupole with integrated strength $2K_{1d}$. This FODO cell ends at another half focusing quadrupole magnet.

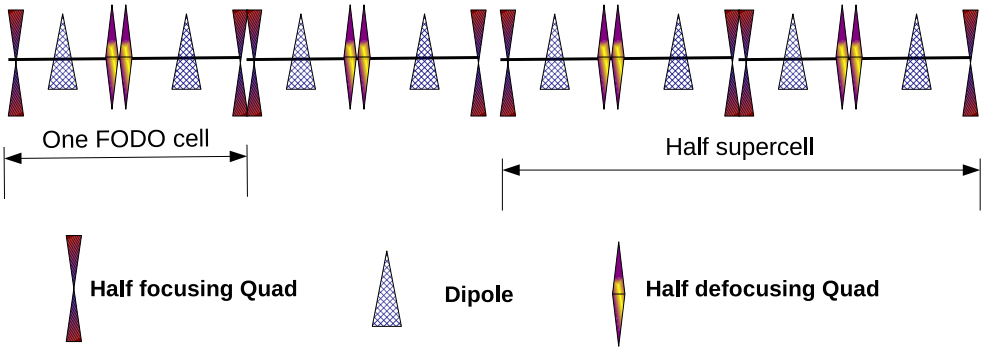

Figure 1: Sketch of one super period of the optics under study.

Applying the matrices approach discussed in the previous section, the overall first order transport matrice of one FODO cell is

$$\mathbf{R}_{FODO} = \mathbf{R_{Qfh}} \cdot \mathbf{R_D} \cdot \mathbf{R_B} \cdot \mathbf{R_D} \cdot \mathbf{R_{QD}} \cdot \mathbf{R_D} \cdot \mathbf{R_B} \cdot \mathbf{R_D} \cdot \mathbf{R_{Qfh}} \tag{39}$$

Under some simplification and thin lens approximation, the 6 by 6 transport matrix $\mathbf{R}_{FODO}$ of this FODO cell can be calculated. Here, in particular, three entries which are the dispersion terms are listed below.

$$\mathbf{R}_{16,FODO} = \left[-4K_{1d}l^2 + (4 - 2K_{1d}\rho\theta)l + \rho\theta\right]\theta \tag{40}$$

$$\mathbf{R}_{26,FODO} = \left[4K_{1d}K_{1f}l^2 + (2K_{1d}K_{1f}\rho\theta - 4K_{1f} - 2K_{1d})l - K_{1f}\rho\theta + 2\right]\theta \tag{41}$$

$$\mathbf{R}_{56,FODO} = 2\left(K_{1d}l^2 - l\right)\theta^2 \tag{42}$$

One need to note that ρ, θ and K_{1f} are all positive, and K_{1d} is negative. Given these conditions, it is obvious to observe that for such a FODO cell: the first order dispersion term $\mathbf{R}_{16,FODO}$ is always positive; the value of the first order angular dispersion term $\mathbf{R}_{26,FODO}$ depends on the choice of ρ, θ, l, K_{1d} and K_{1f}, which can be either positive or negative; the longitudinal first order dispersion term $\mathbf{R}_{56,FODO}$ is always negative.

To illustrate the relations between the dispersion terms and the magnet parameters, here we fix some of the magnets parameters and plot the dispersion terms as a function of K_{1d}, as shown in Figure 2. For the dipole magnet, the bending angle is chosen to be 2.5 degree with a bending radius of $\rho = 4.6m$. The integrated strength of the half focusing quadrupole is $K_{1f} = 1.6$, with a half effective magnetic length of $0.1m$. The drift space length is $l = 0.25m$. As illustrated in Figure 2, for a larger absolute value of K_{1d}, the absolute value of $\mathbf{R}_{16,FODO}$ and $\mathbf{R}_{56,FODO}$ are both larger. At the same time, for given ρ, θ, l, K_{1d} and K_{1f}, there is a unique defocusing quadrupole strength $K_{1d,0}$, to zero the first order angular dispersion $\mathbf{R}_{26,FODO}$ at the end of this FODO cell.

To achieve a first order achromat ($\mathbf{R}_{16} = \mathbf{R}_{26} = 0$) in one supercell as shown in Figure 1, the angular dispersion term $\mathbf{R}_{26}$ has to be zero at the middle point, due to symmetry requirement. This condition can be approximately extended to a zero angular dispersion at the end of the first FODO

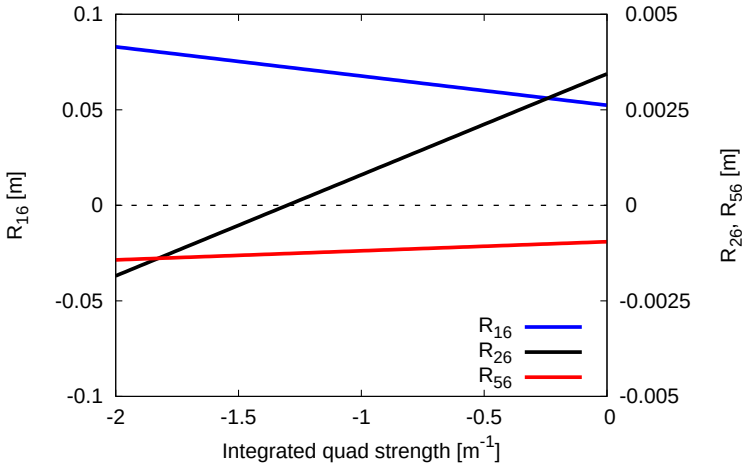

Figure 2: Dispersion terms $\mathbf{R}_{16,FODO}$, $\mathbf{R}_{26,FODO}$ and $\mathbf{R}_{56,FODO}$ of one FODO arc cell, versus the integrated strength of the defocusing quadrupole K_{1d}.

cell, which is the middle point of half supercell. One can then solve the equation and express the required defocusing quadrupole strength as a function of ρ, θ, l and K_{1f}, as shown below.

$$K_{1d} = \frac{4K_{1f}l + K_{1f}\rho\theta - 2}{4K_{1f}l^2 + (2K_{1f}\rho\theta - 2)l} \tag{43}$$

One can calculate the first order transport matrix of a half supercell as shown below, and get a precise solution of $K_{1d,0}$. That is much more complicated and is not discussed in details here.

$$\mathbf{R}_{half,supercell} = \mathbf{R}_{FODO} \cdot \mathbf{R}_{FODO} \tag{44}$$

In designing a lattice, one also needs to constrain the amplitude of the betatron function β in a proper range, which has a maximum and minimum value depending on the cell length and quadrupole strength (for a standard FODO cell), as shown below.

$$\beta\pm = \frac{2(1 \pm \frac{L_{cell}}{4}K_1)}{K_1\sqrt{1 - (\frac{L_{cell}}{4}K_1)^2}} \tag{45}$$

where $\beta\pm$ denotes the maximum and minimum beta functions, L_{cell} the FODO cell length and K_1 the integrated quadrupole strength.

Under the following considerations, an optics is designed as sketched in Figure 1. A dipole magnet with a length of 0.2 m and a bending angle of 2.5 degree is chosen. The drift space length is $l = 0.15m$ for thick quadrupoles which length is $0.2m$. The variation range of the beta functions is constrained between $0.5m$ and $10m$. The quadrupole strengths K_{1d} and K_{1f} are estimated by using formulae (43) and (45), and further optimized by matching in the accelerator design code MAD8 [6]. After optimization, the first order TWISS parameters are shown in Figure 3, where a first order achromat condition is achieved.

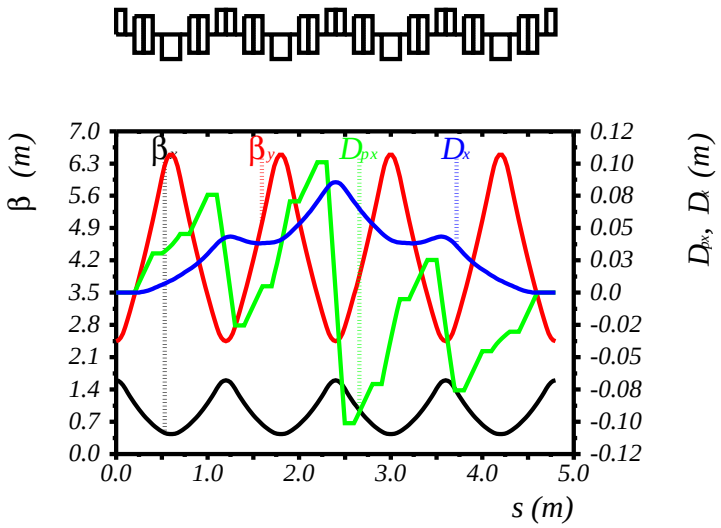

Figure 3: First order dispersion and beta functions of one supercell which consists of four identical FODO cells: black curve denotes horizontal beta function, red curve vertical beta function, blue curve horizontal dispersion function and green curve horizontal angular dispersion function. The color notation is the same for the first order optics in the following figures.

In order to make this supercell extendable, the beta functions need to be identical at the entrance and at the exit. At the same time, the alpha function which is proportional to the derivative of the beta function need to equal zero. The second order horizontal dispersion terms T_{166} and T_{266} are not zero under these constraints. One can then add sextupoles in the optics and zero the second order dispersion.

4 Second order optics

As discussed above, the second order transport matrices of a half supercell can be calculated as in the following formula, which is the multiplication of two identical FODO cell matrices. The second order transport matrix of one FODO cell is the multiplication of the matrices of its subsequent elements, also shown below.

$$\mathbf{T}_{half,supercell} = \mathbf{T}_{FODO} \cdot \mathbf{T}_{FODO} \tag{46}$$

$$\mathbf{T}_{FODO} = \mathbf{T_{Qfh}} \cdot \mathbf{T_D} \cdot \mathbf{T_B} \cdot \mathbf{T_D} \cdot \mathbf{T_{QD}} \cdot \mathbf{T_D} \cdot \mathbf{T_B} \cdot \mathbf{T_D} \cdot \mathbf{T_{Qfh}} \tag{47}$$

Now one can get the expression of the second order dispersion T_{166} and the angular dispersion T_{266}, which are all functions of ρ, θ, l, K_{1d} and K_{1f} (still under thin lens approximation). The detailed expression of T_{166} and T_{266} are more complicated than $\mathbf{R}_{16}$ or $\mathbf{R}_{26}$, so not listed here for simplicity. Similarly as the first order optics, to achieve a second order achromat ($\mathbf{T}_{166} = \mathbf{T}_{266} = 0$)

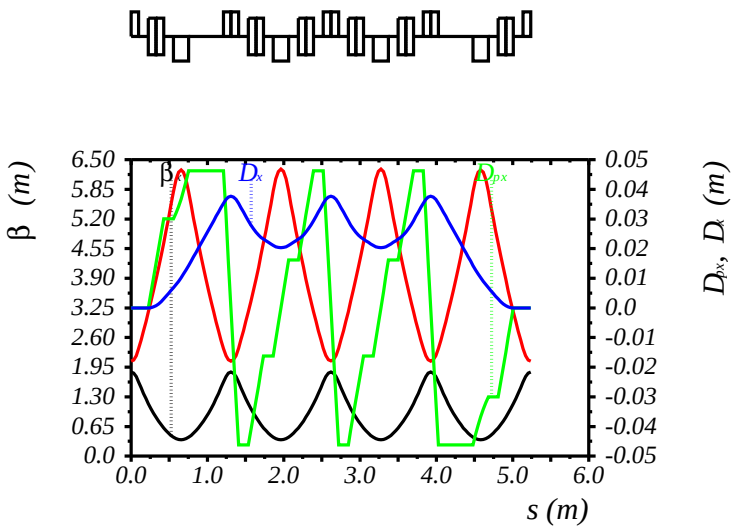

Figure 4: First order dispersion and beta functions of one supercell which consists of four FODO cells, under the missing dipole configuration.

in one supercell as shown in Figure 1, the angular dispersion term $\mathbf{T}_{266}$ has to be zero at the middle point, due to symmetry requirement. For a supercell which consists of four identical FODO cells, this requirement is not easy to fulfill.

However, through some analytical and numerical manipulations, one finds that by adopting the missing dipole option, it is possible to get a second order achromat without the assistance of sextupoles. In the analytical manipulations, a small angle approximation is adopted for the dipole magnet model, and one then has $\sin\theta \approx \theta$ and $\cos\theta \approx 1$. With this treatment, the expression of the second order dispersions T_{166} and T_{266} is simplified and much easier to manipulate. In general a second order achromatic condition is solved by finding parameter relations which fulfill $\mathbf{T}_{266,mid} = 0$ at the middle point of the supercell, and $\mathbf{T}_{166,end} = 0$ at the end of the supercell, plus the first order achromat condition $\mathbf{R}_{26,mid} = 0$ and $\mathbf{R}_{16,end} = 0$. These four expressions ($\mathbf{R}_{26,mid}$, $\mathbf{R}_{16,end}$, $\mathbf{T}_{266,mid}$ and $\mathbf{T}_{166,end}$) are all functions of ρ, θ, l, K_{1d} and K_{1f} (under thin lens approximation). The four zero conditions of the dispersion terms are manipulated analytically using a computer algebra system in MAXIMA [7]. As discussed in details below, one could find reasonable solutions of ρ, θ_1 (θ_2), l, K_{1d} and K_{1f} under the missing dipole configuration. The solution is unique if two of the six variables are fixed. Then these estimated magnet and drift parameters are further matched and optimized in the accelerator design code MAD8 [6], by setting a proper matching constraint (such as $\mathbf{T}_{266} = 0$ at the middle, $\mathbf{T}_{166} = 0$ at the end, reasonable beta functions plus the first order dispersion requirements). The variables ρ, θ_1 (θ_2), l, K_{1d} and K_{1f} are all constrained in a reasonable range.

Under the missing dipole configuration, the second and the seventh dipole are removed in the supercell while the other six dipoles are kept. By slightly modifying the drift length, quadrupole

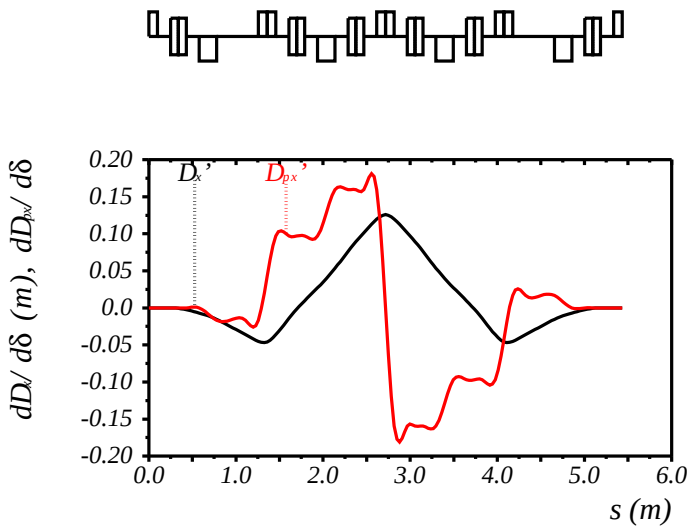

Figure 5: Second order dispersion T_{166} and angular dispersion T_{266} of one supercell which consists of four FODO cells, under the missing dipole configuration.

strength and also the periodic TWISS parameters, one can easily get a first order achromat, as shown in Figure 4. The first order dispersion oscillation along this beamline is different from the one in Figure 3, due to the impact from two missing dipoles. The second order disperison terms T_{166} and T_{266} are much smaller at the end than the previous case, but still not zero.

One possible second order achromat condition is achieved by further slightly adjusting the bending angle of the first and last dipole magnets. At the same time, the quadrupole strength and drift length are also slightly tuned, with the constraints that both first order and second order dispersion terms are zero ($\mathbf{R}_{16} = \mathbf{R}_{26} = 0$ and $\mathbf{T}_{166} = \mathbf{T}_{266} = 0$). That optimization changes the evolution of the second order dispersion and keeps the first order dispersion oscillation similar with the same dipole strength case. The final bending angle of the first and last dipole is chosen to be 1.65 degree each, and it is 1.72 degree each for the other four dipoles in the center two FODO cells. The drift length is minimized and a final length of 0.15 m is achieved. The quadrupole strength is also minimized and the final choice is an integrated strength of -1.6 and +2.6, respectively. The first order optics is almost the same as the one shown in Figure 4. The maximum beta function β_y and dispersion function D_x are 6 m and 0.04 m, respectively.

The evolution of the second order dispersion T_{166} and T_{266} is illustrated in Figure 5, where one observes that the middle point symmetry is always maintained. The maximum absolute value of the second order dispersions is 0.17 m which is relatively small. Notice that for this design either the focusing quadrupoles or the defocusing quadrupoles have the same strength. Here we note that there are also other possible manipulations of this supercell, to achieve a second order achromat, except the missing dipole configuration described here.

In the following section, two application examples using this supercell design is presented. One is

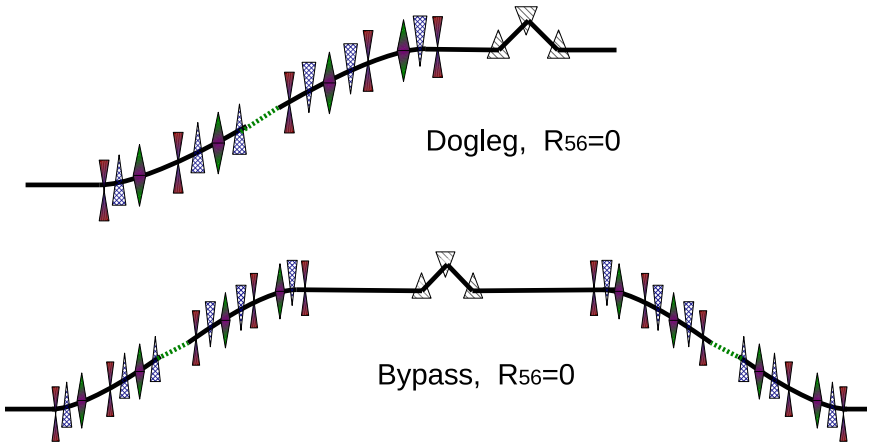

Figure 6: Sketch of a dogleg beamline and a bypass beamline, $R_{56} = 0$ in both cases.

a dogleg beamline design, while the other is a bypass beamline design. Both of these two beamlines are isochronous ($R_{56} = 0$).

5 Possible applications

As discussed above, the beta functions β_x and β_y are symmetric at the two ends of this supercell, and the beta function derivative α equals zero. That feature makes this supercell easy to be extended. Two possible applications are described here, with their sketch shown in Figure 6. In the dogleg beamline, there is one normal supercell followed by a second supercell in which all six dipole magnets switch sign and bend the beam to the opposite direction. This turns the direction of the beamline back (there is an angle due to the first supercell) to the original one, but generates an offset in the bending plane. Using the magnets parameters as specified in the above section, one can do the calculation (matching) and find that each supercell has a first order longitudinal dispersion $R_{56} = 2.5mm$. One can then add a small three (four) dipole chicane after the second supercell, which generates a longitudinal dispersion $R_{56} = -5mm$ and makes the overall system isochronous. There is a small second order longitudinal dispersion T_{566} left on the system which effect should be negligible.

The lower plot in Figure 6 is one possible design of a bypass using these supercells, where one need to shift the beamline with an offset in the bending plane first, then shift it back to the original beamline. Four supercells are employed here to construct this bypass. One may easily flip the two supercells in the dogleg (previous example) and add the flipped one after the small chicane which is in the middle. The middle small chicane also need to be adjusted to provide two times longitudinal dispersion $R_{56} = -10mm$, either by using a stronger dipole or by lengthening the drift length between the dipoles. The length of the straight section in the middle can be lengthened or

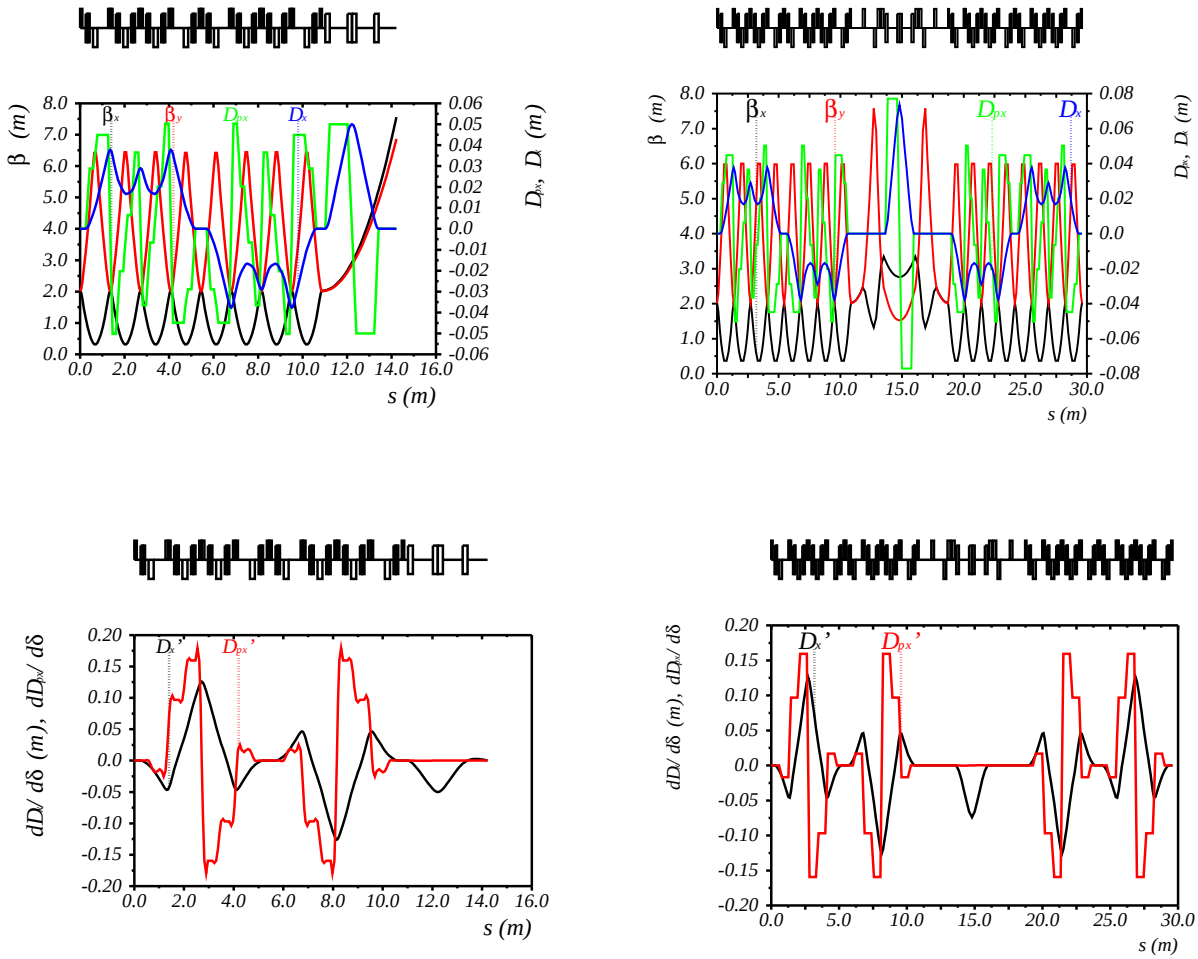

Figure 7: First order and second order optics of a dogleg beamline and a bypass beamline. Left top: First order dispersion and beta functions of the dogleg beamline; Left bottom: Second order dispersion T_{166} and angular dispersion T_{266} of the dogleg beamline; Right top: First order dispersion and beta functions of the bypass beamline; Right bottom: Second order dispersion T_{166} and angular dispersion T_{266} of the bypass beamline.

shortened according to the real constraints, and one only need to add more quadrupoles if a longer straight is necessary.

The first order and second order optics of these two beamlines are matched in MAD8 [6] and presented here in Figure 7. The length of the dogleg beamline is 14 meters, which implies an offset of 1 meter in the bending plane. The offset can be increased by lengthening the drift between the two supercells and one also need to insert several quadrupoles to match the optics there. As mentioned above, the first order longitudinal dispersion $R_{56} = 0$ and there is a small second order dispersion T_{566} left. The length of the bypass beamline is 30 meters in all, where 8 meters is devoted on the middle straight section. Similarly, the offset of 1 meter in the bending plane can be tuned by adjusting the drift length. The length of the middle straight is also easy to tune, to accommodate different beamline elements in a real bypass. A middle plane symmetry is maintained in the bypass beamline and in the two supercells of the dogleg beamline, which is useful in cancelling optics abberations. One may also need to note that the betatron phase advance in the middle straight of the bypass beamline is important in a fine tuning of the system.

The maximum beta function is 8 meters in both beamlines, accompanied by a maximum dispersion $D_x = 0.05m$. The transport matrices elements R_{56} and T_{566}, also the dipole and quadrupole parameters are listed in Table 1 below, assuming a beam energy of $1GeV$. The pole tip field of the dipole and quadrupole magnets is calculated by using the following two formulae, where a half gap of $1.5cm$ is assumed. Note that for higher beam energy one may need to increase the dipole magnets length (current length $0.2m$) to maintain a weaker pole-tip field and partially suppress the incoherent synchrotron radiation effects.

$$B_{dipole} = \frac{B\rho \cdot \theta}{L_{dipole}} \tag{48}$$

$$B_{quad} = K_1 \cdot B\rho \cdot a \tag{49}$$

Table 1: Beamline parameters (at a beam energy of $1GeV$).

$Name$	L [m]	Bend number	θ [d]	B_{dipole} [kG]	B_{quad} [kG]	R_{56} [mm]	T_{566} [mm]
Dogleg	14	16	1.7	4.8	5.4	0	22
Bypass	30	28	1.7	4.8	5.4	0	47

6 Elegant simulation

In order to evaluate the property of these two beamlines in transporting a real beam, the optics described in the above section is converted into the accelerator code Elegant [3]. First of all, the linear and second order optics (all the transport matrices elements) are compared between MAD8 and Elegant, where a good agreement is achieved. Second, a beam which consists of one million macro particles is transported through these two beamlines. Then different beam parameters, such as projected normalized emittance, sliced normalized emittance, sliced energy spread and the longitudinal phase space shape are investigated. A beam of one million macro particles $(x, x', y, y', z, \delta_p)$

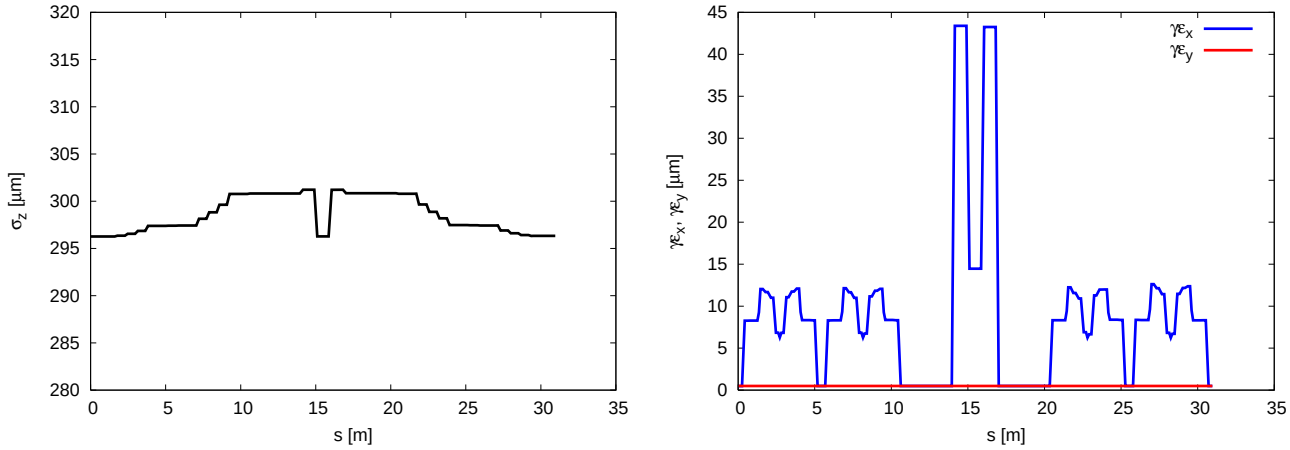

Figure 8: RMS bunch length and projected normalized emittance evolution along the bypass beamline. Left: RMS bunch length; Right: projected normalized emittance.

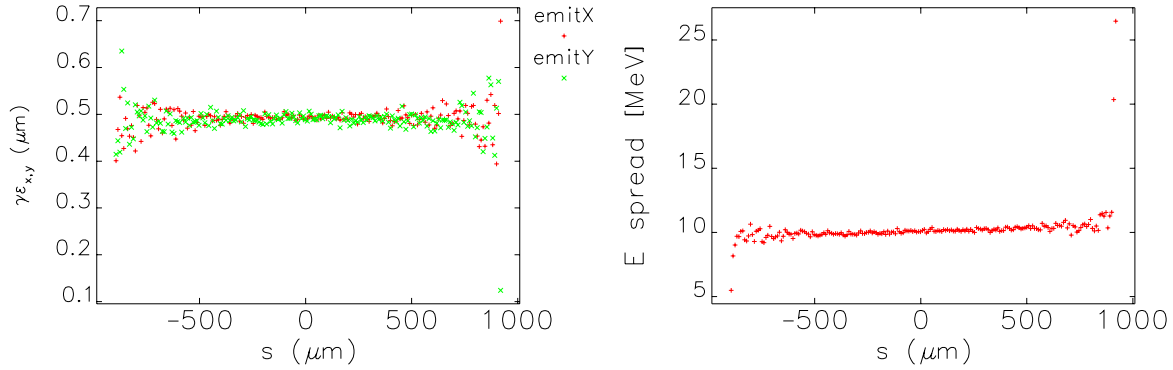

Figure 9: Sliced normalized emittance and energy spread along the longitudinal direction in a bunch. Left: sliced normalized emittance; Right: sliced energy spread.

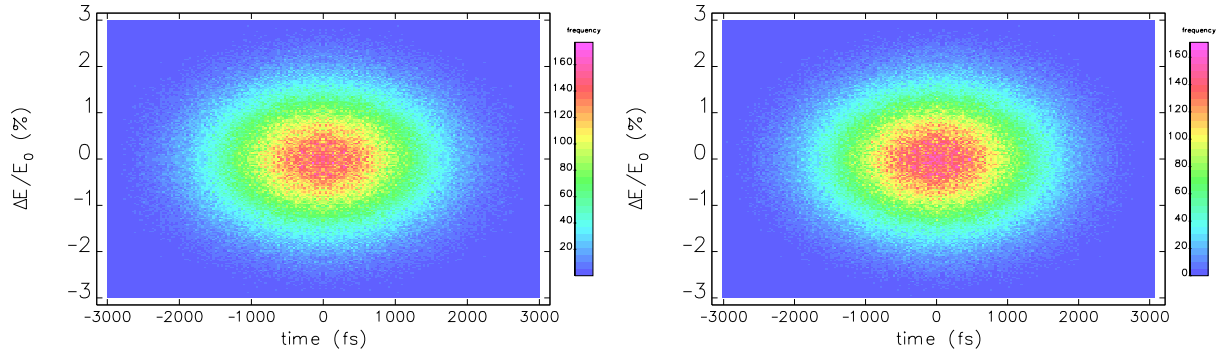

Figure 10: Longitudinal phase space of the beam. Left: initial phase space before injected into the bypass; Right: at the end of the bypass beamline.

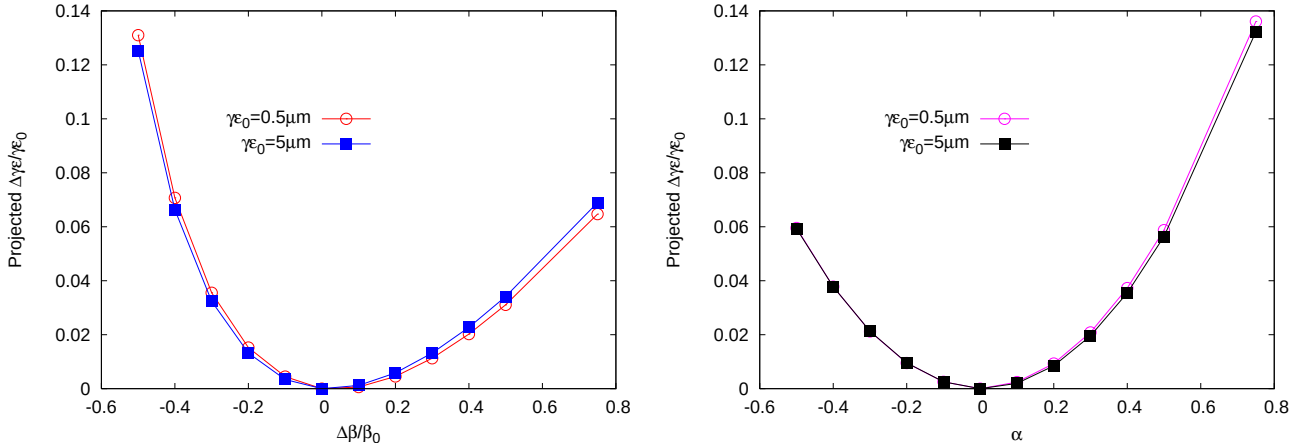

Figure 11: Left: relative change in projected normalized emittance versus the mismatched beta function, for two different emittance, $\gamma\epsilon_x = \gamma\epsilon_y = 0.5\mu m$ and $\gamma\epsilon_x = \gamma\epsilon_y = 5\mu m$. Right: relative change in projected normalized emittance versus initial alpha function when generating the beam.

is generated in Elegant, with an RMS normalized transverse emittance of $\gamma\epsilon_x = \gamma\epsilon_y = 0.5\mu m$, an RMS energy spread of $\sigma_{\delta_p} = 1\%$, an RMS bunch length of $\sigma_z = 300\mu m$ and a beam energy of $1GeV$.

The simulation results of these two beamlines are very similar, and here only the results of the dogleg beamline is presented, for simplicity. The RMS bunch length and projected normalized emittance evolution along the bypass beamline is shown in Figure 8. From Figure 8 (left) one observes that the RMS bunch length changes along the beamline as the summed longitudinal dispersion R_{56} changing. However, at the end of the bypass the initial bunch length is resumed due to a total dispersion $R_{56} = 0$. With a relatively large energy spread of $\sigma_{\delta_p} = 1\%$, this also demonstrates that the effect from small residual second order dispersion T_{566} is negligible. On the other hand, the projected normalized emittance is also preserved through the transport in this beamline, as shown in Figure 8 (right). In the dispersive region between the dipole magnets, the large momentum offset couples into the projected emittance and make it much larger.

Many accelerator applications, for example the Free Electron Laser, concern more on the longitudinally sliced property of the beam, such as emittance and energy spread. The beam which contains one million macro particles is dumped at the end of the bypass beamline, and it is analyzed along its longitudinal direction. The sliced normalized emittance and energy spread along the bunch is shown in Figure 9 (left) and (right). It is demonstrated again that the sliced property of the beam is also preserved. One observes that the slice emittance is $\gamma\epsilon_x = \gamma\epsilon_y = 0.5\mu m$ and the slice energy spread is $10MeV$ ($\sigma_{\delta_p} = 1\%$ at a beam energy of $1GeV$).

The longitudinal phase space is also compared at two different locations in the bypass beamline, say at the injection point and at the end, as shown in Figure 10. Again one observes there is a small deformation on the phase space from the large energy spread and a residual second order dispersion T_{566}. The overall effect of the first order dispersion R_{56} is zero.

Then an initial beam generated from mismatched TWISS parameters (with respect to the optics) is used and the projected emittance evolution is investigated again under this condition. The matched TWISS parameters are from the periodic solution of the supercell discussed above, which are $\beta_{x0} = \beta_{y0} = 2m$ and $\alpha_{x0} = \alpha_{y0} = 0$. An electron beam is generated either by employing

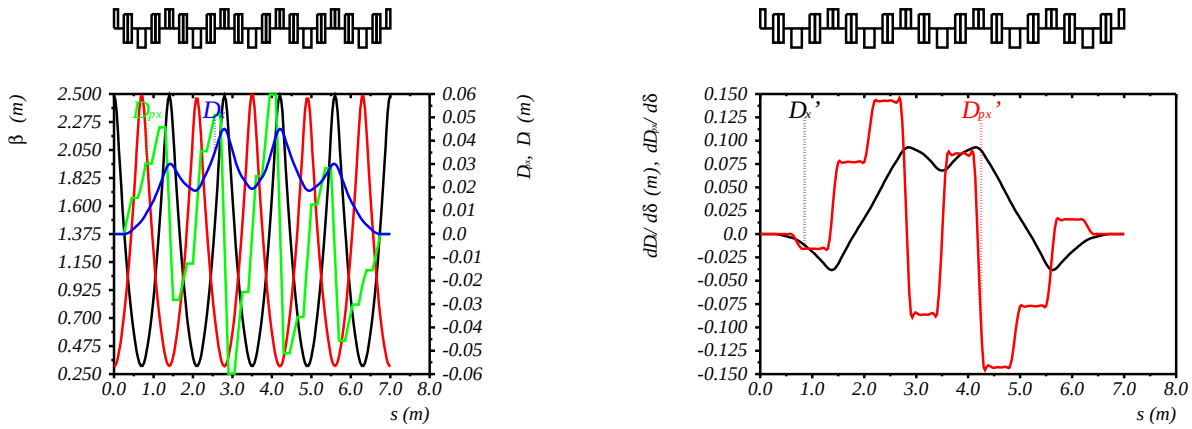

Figure 12: First order and second order optics of a supercell composed of five FODO cells. The horizontal and vertical betatron phase advances are both 90 degree. The four dipole magnets at each end have a bending angle which is roughly a half of the two central dipoles. The dipole strength and phase advance are slightly tuned to generate a second order achromat. Left: First order dispersion and beta functions; Right: Second order dispersion T_{166} and angular dispersion T_{266}.

a mismatched beta function in the bending plane, or taking a mismatched alpha function in the bending plane. An RMS energy spread of $\sigma_{\delta_p} = 1\%$ is again used. The tracking simulation is done with two different transverse beam emittance settings, $\gamma\epsilon_x = \gamma\epsilon_y = 0.5\mu m$ and $\gamma\epsilon_x = \gamma\epsilon_y = 5\mu m$.

The relative variation in projected normalized emittance versus the mismatched beta function is shown in Figure 11. For the case with a mismatched beta function of 50%, the growth in projected emittance is roughly 10%. Within ±20%, the change in projected emittance is negligible. One also need to note that the sliced emittance is preserved much better than the projected emittance. There is no obvious change in slice emittance even with a mismatched beta function of 50%.

7 Conclusion and discussion

A compact supercell is investigated which composes of four FODO arc cells with two missing dipoles. Second order achromat condition is achieved without sextupoles by tuning the strength of the two dipole magnets at two ends. It is proposed to design dogleg or bypass beamlines with these supercells, which can transport an electron beam with large energy spread and preserve its emittance. The elimination of employing sextupoles makes the tolerance on alignment easier to live with. There are also other possible ways to design such supercells with FODO arc cells which may use more dipole and quadrupole magnets. One possible solution is evolved from the classic dispersion suppressor design approach [8], with the first order and second order optics of its supercell shown in Figure 12.

8 Acknowledgement

The author would like to thank M. Woodley, W. Wan, P. Emma, T. Raubenheimer, Z. Huang, J. England, C. Adolphsen and J. Wu for helpful discussions.
This work was supported by the DOE under Contract DE-AC02-76SF00515.

References

[1] K. Brown, IEEE Trans. Nucl. Sci. NS-26 (3), 3490 (1979).

[2] W. Wan and M. Berz, Phys. Rev. E 54, 2870-2883 (1996) .

[3] M. Borland, 'elegant: A Flexible SDDS-Compliant Code for Accelerator Simulation', Advanced Photon Source LS-287, September 2000.

[4] D. Carey, 'The optics of charged particle beams', Hardwood Academic, New York, 1987, page 21-37, page 123-143.

[5] K. Brown, SLAC-R-075, 1982.

[6] H. Grote, F.C. Iselin, The MAD Program (Methodical Accelerator Design) Version 8.15, CERN/SL/90-13 (AP), 1990.

[7] Maxima, a Computer Algebra System, http://maxima.sourceforge.net/.

[8] A. Chao and M. Tigner, Handbook of Accelerator Physics and Engineering, World Scientific, Singapore, page 77 (1998).

A Second order sub matrices

The sub matrices of the second order transport matrix are listed below.

$$\mathbf{T_{x,11}} = \begin{pmatrix} R_{11} & R_{12} & R_{15} & R_{16} \\ R_{21} & R_{22} & R_{25} & R_{26} \\ R_{51} & R_{52} & R_{55} & R_{56} \\ 0 & 0 & R_{65} & 1 \end{pmatrix} \tag{50}$$

$$\mathbf{T_{x,12}} = \begin{pmatrix} T_{111} & T_{112} & T_{115} & T_{116} & T_{122} & T_{125} & T_{126} & T_{155} & T_{156} & T_{166} \\ T_{211} & T_{212} & T_{215} & T_{216} & T_{222} & T_{225} & T_{226} & T_{255} & T_{256} & T_{266} \\ T_{511} & T_{512} & T_{515} & T_{516} & T_{522} & T_{525} & T_{526} & T_{555} & T_{556} & T_{566} \\ 0 & 0 & 0 & 0 & 0 & 0 & 0 & 0 & 0 & 0 \end{pmatrix} \tag{51}$$

$$\mathbf{T_{x,13}} = \begin{pmatrix} T_{133} & T_{134} & T_{144} \\ T_{233} & T_{234} & T_{244} \\ T_{533} & T_{534} & T_{544} \\ 0 & 0 & 0 \end{pmatrix} \tag{52}$$

If one tries to write down every entry in matrix $\mathbf{T_{22,[10\times10]}}$, it reads

$$\mathbf{T_{x,22}} = \begin{pmatrix}
R_{11}^2 & 2R_{11}R_{12} & 2R_{11}R_{15} & 2R_{11}R_{16} & R_{12}^2 & 2R_{12}R_{15} & 2R_{12}R_{16} & R_{15}^2 & 2R_{15}R_{16} & R_{16}^2 \\
R_{11}R_{21} & R_{11}R_{22} & R_{11}R_{25} & R_{11}R_{26} & R_{12}R_{22} & R_{12}R_{25} & R_{12}R_{26} & R_{15}R_{25} & R_{15}R_{26} & R_{16}R_{26} \\
 & +R_{12}R_{21} & +R_{15}R_{21} & +R_{16}R_{21} & & +R_{15}R_{22} & +R_{16}R_{22} & & +R_{16}R_{25} & \\
R_{11}R_{51} & R_{11}R_{52} & R_{11}R_{55} & R_{11}R_{56} & R_{12}R_{52} & R_{12}R_{55} & R_{12}R_{56} & R_{15}R_{55} & R_{15}R_{56} & R_{16}R_{56} \\
 & +R_{12}R_{51} & +R_{15}R_{51} & +R_{16}R_{51} & & +R_{15}R_{52} & +R_{16}R_{52} & & +R_{16}R_{55} & \\
R_{11}R_{61} & R_{11}R_{62} & R_{11}R_{65} & R_{11}R_{66} & R_{12}R_{62} & R_{12}R_{65} & R_{12}R_{66} & R_{15}R_{65} & R_{15}R_{66} & R_{16}R_{66} \\
 & +R_{12}R_{61} & +R_{15}R_{61} & +R_{16}R_{61} & & +R_{15}R_{62} & +R_{16}R_{62} & & +R_{16}R_{65} & \\
R_{21}^2 & 2R_{21}R_{22} & 2R_{21}R_{25} & 2R_{21}R_{26} & R_{22}^2 & 2R_{22}R_{25} & 2R_{22}R_{26} & R_{25}^2 & 2R_{25}R_{26} & R_{26}^2 \\
R_{21}R_{51} & R_{21}R_{52} & R_{21}R_{55} & R_{21}R_{56} & R_{22}R_{52} & R_{22}R_{55} & R_{22}R_{56} & R_{25}R_{55} & R_{25}R_{56} & R_{26}R_{56} \\
 & +R_{22}R_{51} & +R_{25}R_{51} & +R_{26}R_{51} & & +R_{25}R_{52} & +R_{26}R_{52} & & +R_{26}R_{55} & \\
R_{21}R_{61} & R_{21}R_{62} & R_{21}R_{65} & R_{21}R_{66} & R_{22}R_{62} & R_{22}R_{65} & R_{22}R_{66} & R_{25}R_{65} & R_{25}R_{66} & R_{26}R_{66} \\
 & +R_{22}R_{61} & +R_{25}R_{61} & +R_{26}R_{61} & & +R_{25}R_{62} & +R_{26}R_{62} & & +R_{26}R_{65} & \\
R_{51}^2 & 2R_{51}R_{52} & 2R_{51}R_{55} & 2R_{51}R_{56} & R_{52}^2 & 2R_{52}R_{55} & 2R_{52}R_{56} & R_{55}^2 & 2R_{55}R_{56} & R_{56}^2 \\
R_{51}R_{61} & R_{51}R_{62} & R_{51}R_{65} & R_{51}R_{66} & R_{52}R_{62} & R_{52}R_{65} & R_{52}R_{66} & R_{55}R_{65} & R_{55}R_{66} & R_{56}R_{66} \\
 & +R_{52}R_{61} & +R_{55}R_{61} & +R_{56}R_{61} & & +R_{55}R_{62} & +R_{56}R_{62} & & +R_{56}R_{65} & \\
R_{61}^2 & 2R_{61}R_{62} & 2R_{61}R_{65} & 2R_{61}R_{66} & R_{62}^2 & 2R_{62}R_{65} & 2R_{62}R_{66} & R_{65}^2 & 2R_{65}R_{66} & R_{66}^2
\end{pmatrix} \tag{53}$$

$$\mathbf{T_{x,33}} = \begin{pmatrix}
R_{33}^2 & 2R_{33}R_{34} & R_{34}^2 \\
R_{33}R_{43} & R_{33}R_{44} + R_{34}R_{43} & R_{34}R_{44} \\
R_{43}^2 & 2R_{43}R_{44} & R_{44}^2
\end{pmatrix} \tag{54}$$